JOURNAL OF VIROLOGY, July 1993, p. 4214–4226
0022-538X/93/074214-13$02.00/0
Copyright © 1993, American Society for Microbiology
Vol. 67, No. 7

Importance of Interferons in Recovery from Mousepox

GUNASEGARAN KARUPIAH,[1] TORGNY N. FREDRICKSON,[2] KEVIN L. HOLMES,[3] L. H. KHAIRALLAH,[4] AND R. MARK L. BULLER[1]*

Laboratory of Viral Diseases[1] and Biological Resources Branch,[3] National Institute of Allergy and Infectious Diseases, and Registry of Experimental Cancers, National Cancer Institute,[2] Bethesda, Maryland 20892, and Department of Physiology and Neurobiology, University of Connecticut, Storrs, Connecticut 06292[4]

Received 14 December 1992/Accepted 29 March 1993

Gamma interferon is shown to be critical in recovery of C57BL/6 mice from mousepox. Anti-gamma interferon treatment of mice infected in the footpad with ectromelia virus resulted in enhanced spread to and efficient virus replication in the spleen, lungs, ovaries, and, especially, liver. All treated, infected mice died within a mean of 7 days, 2.5 days earlier than mice with severe combined immunodeficiency that were given a comparable infection. On the other hand, alpha interferon appeared not to have a major role in controlling virus replication in tissues examined, and beta interferon was important for virus clearance in the liver and ovaries but not the spleen. Either anti-alpha, beta interferon or anti-beta interferon antibody therapy resulted in only 25% mortality. Infected control mice survived but showed persistence of ectromelia virus at the site of infection (the footpad) and transient presence of the virus in the spleen, liver, lungs, and ovaries and in the fibroreticular but not lymphoid cells of the draining popliteal lymph node. Depletion of gamma interferon but not alpha and/or beta interferon resulted in a significant reduction in the numbers of splenic T (especially γδ-TCR$^+$), B, and Mac-1$^+$ cells, although the proportion of Mac-1$^+$ cells in the spleen increased compared with control values. Depletion of alpha, beta, or gamma interferons did not severely affect the generation of virus-specific cytotoxic T-lymphocyte responses or natural killer cell cytolytic activity. This study, in which a natural virus disease model was used, underscores the crucial importance of gamma interferon in virus clearance at all stages of infection and in all tissues tested except the primary site of infection, where virus clearance appears to be delayed.

Ectromelia virus (EV), the causative agent of mousepox, has been used extensively in the past as an experimental model for studies of pathogenesis of generalized viral infections and viral immunology (5, 9a). Fenner established that the natural route of infection through skin abrasions, especially in the feet, tail, or nose, could be mimicked with a low dose of virus in the footpad (f.p.) of the mouse (9). When this route of inoculation is used, virus typically replicates in the epidermal and dermal cells and subsequently spreads from the skin lesion to draining lymph nodes (LNs). In susceptible strains of mice (A, BALB/c), death by 6 to 7 days postinfection (p.i.) results from disseminated infection in the liver and spleen with resultant necrosis. In contrast, virus spread is slower in genetically resistant strains (C57BL/6, AKR), with lower levels of infectivity in the liver and spleen, causing minimal, nonfatal lesions (5, 9a). Although resistance to mousepox is not fully understood and depends on the infection route, virulence of the virus, and mouse genotype (5), studies with C57BL mice indicate that certain of the non-*H-2*-linked resistance genes act through a radioresistant cell(s) or factor(s) and are operative before generation of virus-specific cytotoxic T lymphocytes (CTL) (22). In addition, chimera experiments have shown that *H-2*-linked genes influence resistance through radiosensitive lymphoid cells (23), and a crucial role for T cells with cytotoxic activity (CTL) has long been known (16, 24). As shown by cell depletion procedures, blood monocytes as well as tissue-fixed macrophages also play important roles in mediating the early resistance to EV-induced severe disease (3, 39). Recent studies (11) have also indicated that type I (alpha and beta) interferons (IFN-α and IFN-β) and natural killer (NK) cells may contribute to the host antiviral responses, mediating resistance to a large dose of intravenously administered EV in C57BL mice. Similarly, type II (gamma) IFN (IFN-γ) has been shown to be important for the elimination of intravenously administered vaccinia virus (VV) (13, 18, 31), an orthopoxvirus closely related to EV.

The goal of this study was to determine the relative importance of IFN-α, IFN-β, and IFN-γ in recovery from EV f.p. infection of the disease-resistant C57BL/6 mouse. Because most cells express IFN receptors and IFNs are capable of activating or inhibiting a wide range of cellular and immunological functions (26, 32), IFNs are able to affect many different phases of the host response to infection, including (but not limited to) the induction of an antiviral state within cells at risk of virus infection. Using anti-IFN antibody depletion therapy, we have used a number of approaches to examine the importance of IFNs in recovery from mousepox at various stages of the disease in several different tissues. Virus recovery and histologic, ultrastructural, and in situ hybridization analyses of infected tissues were used to measure pathological changes, and flow cytometry and functional tests for NK cell and CTL activities determined whether IFN depletion had any effect on cell-mediated responses to infection.

MATERIALS AND METHODS

Mice. Specific-pathogen-free female C57BL/6NCR (B6) (*H-2^b*) mice (Charles River Laboratories, Wilmington, Mass., procured through the National Cancer Institute, Frederick, Md.) were used at 6 to 10 weeks of age.

Viruses. Plaque-purified EV (Moscow strain), designated Mos-3-P_2, was propagated in murine L929 cells and purified as described previously (7). The virus titer was determined

* Corresponding author.

by using BS-C-1 cell monolayers. The WR strain of VV (VV-WR) propagated in BS-C-1 cells was used to infect target cells for cytotoxicity assays. The New Jersey strain of vesicular stomatitis virus propagated in Vero cells was kindly provided by A. Hügin, Laboratory of Immunopathology, National Institute of Allergy and Infectious Diseases. Supernatants from vesicular stomatitis virus-infected Vero cell cultures were used as a source of stock virus.

Cell lines. L929, a continuous fibroblast line from the C3H mouse; YAC-1, a line derived from Moloney murine leukemia virus-induced lymphoma in the A/Sn mouse; and BS-C-1, a continuous African green monkey kidney cell line, were maintained in Eagle's minimum essential medium (Quality Biological, Inc., Gaithersburg, Md.) supplemented with L-glutamine, antibiotics, and 10% fetal calf serum, hereafter referred to as complete medium. MC-57G ($H\text{-}2^b$), a fibroblast line derived from the B6 mouse, was maintained in Iscove's modified Dulbecco's minimal essential medium (GIBCO, Grand Island, N.Y.) supplemented with 1 mM *N*-2-hydroxyethylpiperazine-*N'*-2-ethanesulfonic acid (HEPES), L-glutamine, antibiotics, and 10% fetal calf serum.

IFNs, anti-IFN antibodies, and control IgG. The activity of purified murine IFN-β (lot 83053) and muIFN-αβ (lot 83052) (Lee Bimolecular Research Laboratories, Inc., San Diego, Calif.) had been established by the manufacturer by using comparative assays with IFN reference reagents provided by the Antiviral Substances Program, National Institute of Allergy and Infectious diseases. Recombinant murine IFN-γ (lot M3-RD38; specific activity, 5.2×10^6 U/ml; concentration, 1.1 mg/ml) was a generous gift of Genentech Inc., South San Francisco, Calif.

Rabbit antisera to murine IFN-αβ (lot 88098) and murine IFN-β (lot 88099) and rabbit preimmune control sera (lot 90032) were also obtained from Lee Bimolecular Research Laboratories. Since an antibody to murine IFN-α was not easily available, we used instead a rabbit antiserum to murine IFN-αβ. Affinity-purified rabbit polyclonal antibody to murine IFN-γ was a gift of G. Chaudhri, Surgery Branch, National Cancer Institute. A hybridoma line, secreting neutralizing monoclonal antibody (MAb) to murine IFN-γ (rat immunoglobulin G1 [IgG1]; clone XMG-6), was obtained from H. C. Morse III, Laboratory of Immunopathology, National Institute of Allergy and Infectious Diseases, and purified by ammonium sulfate precipitation from ascites fluid. Purified rat and rabbit IgG (Calbiochem Corp., La Jolla, Calif.) were dialyzed extensively in phosphate-buffered saline (PBS) to remove sodium azide used as a preservative and filter sterilized before use.

Determination of anti-IFN antibody-neutralizing activity. The neutralizing titer of each antiserum or MAb was determined essentially by the method of Spitalny and Havell (35). The neutralizing activity of the anti-IFN antibodies was specific in that only the homologous IFN was neutralized. One neutralizing unit is defined as the reciprocal of the dilution of antibody which completely neutralizes 10 U of the corresponding IFN activity. On the basis of a pilot experiment, 100 U of neutralizing activity was determined as the standard dose for injection into mice.

Cytotoxicity assays. The standard chromium-51 release assays were performed to measure CTL and NK cell responses, as described in detail elsewhere (14).

Depletion of effector cell suspensions with antibody and complement. The following antisera and MAbs were used as described previously (14) at the dilutions indicated for in vitro cell depletion with complement for phenotypic analysis: anti-Thy-1.2 (clone F7D5; Serotec Ltd., Blackthorn Bicester, England) at a dilution of 1/1,000; anti-CD4 (clone RL174) and anti-CD8 (clone 3.155) at dilutions of 1/2; and rabbit anti-asialo-GM_1 (Wako Pure Chemicals USA, Inc., Richmond, Va.) at a dilution of 1/50. Low-toxicity rabbit complement (Cedarlane Laboratories Ltd., Hornby, Ontario, Canada) was used at a final dilution of 1/10.

Flow cytometry. The following fluorochrome-conjugated MAbs were used for single- and two-color analysis as described previously (14): phycoerythrin-conjugated anti-CD4 (clone GK 1.5; Becton Dickinson, Mountain View, Calif.), fluorescein isothiocyanate (FITC)-conjugated anti-CD8 (clone 53.6.7; Becton Dickinson), FITC-conjugated anti-αβ-TCR (clone H57-597; Pharmingen, San Diego, Calif.), FITC-conjugated anti-γδ-TCR (clone GL3; Pharmingen), FITC-conjugated anti-IgM (clone LO-MM-9; Zymed, San Francisco, Calif.), FITC-conjugated anti-B220 (clone RA3-6B2), FITC-conjugated anti-Mac-1 (clone M1/70), FITC-conjugated Thy-1.2 (clone 30-H12; Becton Dickinson), and biotinylated anti-CD3-ε (clone 145-2C11). For Thy-1.2 staining, cells were incubated with 5 μg of anti-FcγII receptor MAb (clone 2.4G2) for 15 min prior to the addition of anti-Thy-1.2. Dead cells were gated out by uptake of propidium iodide. For each sample, 20,000 events were collected and analyzed on a FACS 440 flow cytometer (Becton Dickinson Immunocytometry Systems, San Jose, Calif.).

Histology. Tissues were fixed in Tellyesniczky's acetic acid-ethanol-formalin solution, embedded in paraffin, sectioned into 4-μm sections, and stained with hematoxylin and eosin before being examined with a light microscope. For electron microscopy, popliteal LNs were fixed for 3 h in 2.5% glutaraldehyde in Millonig's sodium phosphate buffer (pH 7.9) and stored at 4°C in the same buffer lacking glutaraldehyde until needed for processing for electron microscopy.

In situ hybridization. Sections (4 μm) were deparaffinized and hybridized at room temperature for 2 h with a biotinylated EV genomic DNA probe made from DNA isolated from purified virions. Hybrids were detected with a streptavidin-alkaline phosphatase developing system (Bethesda Research Laboratories Inc., Gaithersburg, Md.), and tissues were counterstained with nuclear fast red.

Determination of virus titers in liver, spleen, lungs, ovaries, popliteal LNs, and f.p. Tissues removed aseptically from mice infected with EV were weighed and snap-frozen at −70°C. Virus infectivity was assayed as described previously and is expressed as $\log_{10}$ PFU per gram of tissue (7).

Virus infection and in vivo treatment of mice with anti-IFN antibodies. Groups of mice were given intraperitoneal injections of 100 neutralizing units of the appropriate anti-IFN or control antibody diluted in PBS or PBS alone 1 day before infection (day −1), on the day of infection (day 0), and every day thereafter until 1 day before sacrifice. Mice were inoculated subcutaneously in the right f.p. with 4×10^3 PFU of EV in 20 μl of PBS and were killed at various times. Tissues were taken for determination of viral infectivity in organs, histopathology, frequencies of specific cell types in the spleen, and/or splenic NK cell and CTL responses. For controls, concentrations of the rat IgG, rabbit IgG, or preimmune serum were matched with those of rat MAb (anti-IFN-γ) and polyclonal rabbit antisera (anti-IFN-αβ, anti-IFN-β, and anti-IFN-γ).

TABLE 1. Effect of anti-IFN antibodies on the survival of C57BL/6 mice infected with EV

Group	Virus and treatment[a]	Mortality (no. dead/ total no.)[b]	MTD (days)[c]
A	Control (no EV or anti-IFN)	0/4	
B	Anti-IFN-αβ only	0/4	
C	Anti-IFN-β only	0/4	
D	Anti-IFN-γ only	0/4	
E	EV only	0/4	
F	EV + rat IgG	0/4	
G	EV + rabbit IgG	0/4	
H	EV + anti-IFN-αβ	1/4	12
I	EV + anti-IFN-β	1/4	10
J	EV + anti-IFN-γ (rat)	22/22[d]	7
K	EV + anti-IFN-γ (rabbit)	6/6[d]	7.2

[a] Experimental design as in Materials and Methods. All surviving mice were sacrificed on day 14.

[b] The livers of infected B6 mice treated with anti-IFN-β or anti-IFN-γ contained more than 8.0 $\log_{10}$ PFU of virus, consistent with a viral cause of death, whereas the liver from the mouse treated with anti-IFN-αβ showed less than 2.0 $\log_{10}$ PFU. The cause of death of this mouse remains questionable.

[c] MTD, mean time to death for all deaths in all experiments.

[d] Data from two separate experiments.

RESULTS

Effect of anti-IFN antibodies on morbidity and mortality of EV-infected B6 mice. Groups of four B6 mice were treated with 100 neutralizing units of antibodies to IFNs, control IgGs, or PBS and mock infected or infected by the f.p. route with EV. Mortality and morbidity (hunched posture or ruffled fur) were monitored for a 14-day period. Treatment of control mice with antibodies to IFN-αβ, IFN-β, or IFN-γ (Table 1, groups B to D) and treatment of infected mice with nonspecific rat or rabbit IgG (groups F and G) had no effect on the health status of the animals; however, EV-infected mice that had been given antibodies to IFN-αβ (group H) or IFN-β (group I) showed morbidity by day 6. One anti-IFN-αβ- and one anti-IFN-β-treated mouse died on days 12 and 10 post-infection (p.i.), respectively. By day 14, the remaining anti-IFN-αβ and anti-IFN-β treated mice remained healthy. In contrast, all mice infected with EV and treated with either rat MAb or rabbit polyclonal antibody to IFN-γ (groups J and K) showed obvious signs of morbidity by day 5 and were dead by day 7 p.i., with greater than 8 $\log_{10}$ PFU of virus recovered from the liver. For comparison, a similar EV infection of untreated mice with severe combined immunodeficiency (strain C.B.17) resulted in 100% mortality and mean time to death of 9.5 days (data not shown).

Effect of anti-IFN antibody on EV replication at various times after infection of B6 mice. To determine the effect of various antibody treatments on the kinetics of virus replication in different tissues, groups of B6 mice were treated and infected for 1, 3, 5, and 14 days, at which time three mice from each group were sacrificed and the virus infectivity for several organs was determined (Table 2). No virus infectivity was found in the liver, spleen, lungs, or ovaries at day 1 p.i. (data not shown).

Control rat and rabbit IgG treatments of infected B6 mice resulted in tissue infectivity levels which were usually indistinguishable from those in untreated, infected B6 mice and, except in one case (rat IgG and spleen), were below the limit of detection by day 14 p.i. Treatment with anti-IFN-αβ or anti-IFN-β resulted in a significant increase in levels of virus infectivity in the spleen, liver, and ovaries but not the lungs at day 5 p.i. compared with controls. By day 14 p.i. virus infectivity was undetectable in lung tissue, significantly reduced in spleen tissues, and increased in liver and ovary tissues. Treatment of infected mice with anti-IFN-γ resulted in an earlier detection of virus in the spleen and lungs and in increasing levels of virus infectivity in all organs examined until the death of the animal.

Regardless of the antibody treatments, virus infectivity levels in the popliteal LNs at day 5 p.i. or in the f.p. at day 14 p.i. were very similar. This may indicate that virus replication in these tissues is not sensitive to IFN-mediated effects or that the antibodies, which were administered by the i.p. route, did not traffic well to the f.p. or popliteal LN. To differentiate between these possibilities, B6 mice were treated by the f.p. route with anti-IFN antibody before and after EV infection by the same route. Virus infectivity levels in f.p. and liver tissues from mice sacrificed at days 3 and 5 p.i. are presented in Table 3. Administration of anti-IFN-αβ, anti-IFN-β, or anti-IFN-γ or a mixture of anti-IFN-αβ and anti-IFN-γ antibodies into the f.p. resulted in no effect on virus infectivity levels at day 3 and the detection of less than 1 $\log_{10}$ PFU of additional virus in the f.p. compared with controls at day 5 ($P < 0.001$, Student's t test). The detection of an additional 3 $\log_{10}$ PFU in liver tissue at day 5 p.i. from anti-IFN-γ-treated mice compared with untreated controls indicated that administration of this MAb by the f.p. route was as effective as the intraperitoneal route for systemic inhibition of IFN effects (compare Table 3 with Table 2, liver, day 5). The reason for the differences between the EV infectivity values obtained following treatment with anti-IFNαβ and anti-IFN-β in f.p. or liver at day 5 p.i. is not clearly understood. Taken together, these results suggested that (i) EV replication in the f.p. and popliteal LNs was far less sensitive to IFN-mediated antiviral effects than was EV replication the liver, spleen, and ovaries; (ii) comparisons of the results obtained with anti-IFN-αβ and anti-IFN-β suggested that IFN-α was not acting alone or in synergy with IFN-β to reduce EV infectivity in assayed organs in a biologically significant manner; (iii) IFN-β was important for virus clearance from the liver and ovaries; and (iv) IFN-γ was important for virus clearance from all tissues tested.

Light microscopy. Popliteal LNs, liver, lungs, and spleen from B6 mice treated daily with anti-IFN antibody throughout a 7-day infection period were examined by light microscopy (Table 4). Mice receiving EV alone showed tissue responses confined to the draining popliteal LNs, which varied from reactive (which was detectable by day 2 p.i.) to focal necrosis in the subcapsular cortical area (detectable by day 4 p.i.) (data not shown). At day 7 p.i. in mice which showed LN necrosis, neutrophilic infiltration within the area of necrosis was moderately severe and increased lymphoid cellularity was seen in nonnecrotic areas (Fig. 1A; mouse 1684). There were no detectable lesions in the liver, spleen, or lungs in untreated, EV-infected B6 mice.

In mice given anti-IFN treatments, lesions were detected in the popliteal LNs, liver, and spleen. Among LNs, the degree of necrosis varied from focal with only a moderately larger area affected than for the control (Fig. 1B; mouse 1692) to necrosis of the entire node (Fig. 1C; mouse 1691). A similar gradation of necrosis was seen in livers, varying from small, widely scattered areas containing mononuclear cells (Fig. 1D; mouse 1694) to almost complete necrosis of the hepatic parenchyma (Fig. 1E; mouse 1693). Generally the spleen was not severely involved, and in most cases the only changes seen were moderate reactivity in the red pulp with erythropoiesis and granulocytopoiesis accompanied by moderate congestion of erythrocytes within sinusoids, consistent

TABLE 2. Effect of anti-IFN antibodies on EV replication in various tissues

Organ	Virus and treatment[a]	Log_{10} virus titers ± SEM[b] on[c]:		
		Day 3[d]	Day 5	Day 14[e]
Liver	EV only	≤ 2.0	5.0 ± 0.4	≤ 2.0
	EV + rat IgG	≤ 2.0	5.1 ± 0.6	≤ 2.0
	EV + rabbit IgG	≤ 2.0	5.1 ± 0.3	≤ 2.0
	EV + anti-IFN-αβ	**3.1 ± 0.3**	**6.3 ± 0.6**	**6.9 ± 0.1**
	EV + anti-IFN-β	2.1 ± 1.3	**6.1 ± 0.5**	**6.3 ± 0.8**
	EV + anti-IFN-γ (rat)	**3.8 ± 0.3**	**7.2 ± 0.4**	—[f]
Spleen	EV only	≤ 2.0	4.3 ± 0.3	≤ 2.0
	EV + rat IgG	≤ 2.0	4.7 ± 0.5	2.6 ± 1.9
	EV + rabbit IgG	≤ 2.0	4.9 ± 0.4	≤ 2.0
	EV + anti-IFN-αβ	2.5 ± 1.0	**6.7 ± 0.7**	3.5 ± 0.2
	EV + anti-IFN-β	≤ 2.0	**6.5 ± 0.3**	≤ 2.0
	EV + anti-IFN-γ (rat)	**4.3 ± 0.9**	**8.3 ± 0.4**	—
Lung	EV only	≤ 2.0	3.4 ± 0.2	≤ 2.0
	EV + rat IgG	≤ 2.0	3.8 ± 0.2	≤ 2.0
	EV + rabbit IgG	≤ 2.0	3.1 ± 0.7	≤ 2.0
	EV + anti-IFN-αβ	≤ 2.0	4.8 ± 0.2	≤ 2.0
	EV + anti-IFN-β	≤ 2.0	4.5 ± 0.4	≤ 2.0
	EV + anti-IFN-γ (rat)	≤ 2.0	**6.6 ± 0.4**	—
Ovary	EV only	≤ 1.0	3.4 ± 0.3	≤ 1.0
	EV + rat IgG	≤ 1.0	3.3 ± 0.3	≤ 1.0
	EV + rabbit IgG	≤ 1.0	3.1 ± 0.2	≤ 1.0
	EV + anti-IFN-αβ	≤ 1.0	**4.5 ± 0.2**	**6.9 ± 0.1**
	EV + anti-IFN-β	≤ 1.0	**4.3 ± 0.5**	**6.3 ± 0.8**
	EV + anti-IFN-γ (rat)	≤ 1.0	**5.5 ± 0.6**	—
Popliteal LN	EV only	6.0 ± 0.6	7.6 ± 0.1	5.2 ± 0.7[h]
	EV + rat IgG	ND[g]	7.4 ± 0.1	ND
	EV + rabbit IgG	ND	7.1 ± 0.8	ND
	EV + anti-IFN-αβ	ND	7.6 ± 0.1	ND
	EV + anti-IFN-β	ND	7.9 ± 0.4	ND
	EV + anti-IFN-γ (rat)	ND	7.8 ± 0.3	ND
Footpad	EV only	ND	ND	8.4 ± 0.5
	EV + rat IgG	ND	ND	8.9 ± 0.2
	EV + rabbit IgG	ND	ND	8.9 ± 0.3
	EV + anti-IFN-αβ	ND	ND	8.6 ± 0.6
	EV + anti-IFN-β	ND	ND	8.4 ± 0.4
	EV + anti-IFN-γ (rat)	ND	ND	—

[a] Experimental design as in Materials and Methods.
[b] SEM, standard error of the mean.
[c] Boldface type represents significance by Student's t test ($P < 0.05$ to $P < 0.0001$).
[d] No virus infectivity was detected from tissues from mice sacrificed on day 1.
[e] All surviving mice were sacrificed on day 14.
[f] All infected mice treated with anti-IFN-γ died on day 7 p.i.
[g] ND, not done.
[h] Value from day 12.

with an inflammatory reaction (Table 4). The exception to this response was the moderate to severe necrosis, involving all components of the spleen, seen in mice treated with anti-IFN-γ (Fig. 1F; mouse 1693) along with severe necrosis in the LNs and liver, representing the most advanced cases observed in this study. This severe pathologic response was representative of what would be expected in susceptible A strain mice receiving a similar dose of virus (data not shown). No lesions were observed in lungs from mice undergoing any of the treatments.

In situ hybridization for EV DNA. Virus replication as indicated by cells containing large amounts of virus DNA was generally confined to the necrotic areas, as detected by light microscopy. In the liver, hepatocytes were the major cell type to react with the EV DNA probe, and widespread

TABLE 3. Effect of anti-IFN antibody injections in the f.p. on EV infectivity levels in the f.p. and liver

Treatment[a]	Log_{10} virus titers ± SEM[b] on[c]:		
	Day 3 p.i. (f.p.)	Day 5 p.i.	
		f.p.	Liver
EV only	6.3 ± 0.3	6.8 ± 0.1	4.9 ± 0.1
EV + anti-IFN-αβ	6.6 ± 0.1	6.8 ± 0.1	**6.3 ± 0.1**
EV + anti-IFN-β	6.5 ± 0.2	**7.7 ± 0.1**	5.4 ± 0.4
EV + anti-IFN-γ	6.4 ± 0.3	**7.6 ± 0.2**	**7.9 ± 0.6**
EV + anti-IFN-αβ + anti-IFN-γ	6.3 ± 0.4	**7.5 ± 0.1**	**7.7 ± 1.0**

[a] Mice were treated and infected as described in Materials and Methods.
[b] SEM, standard error of the mean.
[c] Boldface type represents significance ($P < 0.001$; Student's t test).

TABLE 4. Histopathology of tissue from EV-infected and anti-IFN antibody-treated C57BL/6 mice on day 7 p.i.

Virus and treatment[a,b]	Mouse	Histopathology of[c]:		
		Popliteal LN	Liver	Spleen
EV only	1683	R+	—[d]	—
	1684	N+	—	ND[e]
EV + anti-IFN-αβ	1687	—	N+++	N+
	1688	R++	N+	R+
	1689	N++	N+	R++
EV + anti-IFN-β	1690	R+	N+	R+
	1691	N++++	N+++	R+
	1692	N+++	N++	R+
EV + anti-IFN-γ (rat MAb)	1693	ND	N+++	N++++
	1694	N++++	N++	N++

[a] All mice were infected and treated as described in Materials and Methods.
[b] Anti-IFN antibody-treated or -untreated mock-infected mice showed no detectable lesions.
[c] R, reactive (increased cellularity in LN or splenic white pulp with follicular enlargement with increased mitotic activity in follicles); N, necrosis (from restricted [focal] necrosis with an otherwise intact organ [+] to severe necrosis with total destruction of the organ [++++]).
[d] —, normal.
[e] ND, not done.

intense staining was seen in areas with advanced necrosis (Fig. 2A). Staining of hepatocytes within necrotic foci was either intense and focal or diffuse (Fig. 2B). Virus DNA was rarely detected in cells within necrotic splenic tissue, and it seemed to be restricted to fibroreticulum-like cells (Fig. 2C). A somewhat similar hybridization pattern was seen for the popliteal LNs, in which scattered EV DNA-positive fibroreticulum-like cells were seen in the sharply demarcated zone of necrosis (Fig. 2D). It was not clear why there were so few positive cells, considering the extent of the necrosis.

The severity of the tissue lesions observed in each treatment group (Table 4; Fig. 1 and 2) correlated with EV replication as shown by levels of virus infectivity (Table 2), except for the day 5 p.i. value for LNs from mice receiving no antibody treatment. These tissues contained more than 7 $\log_{10}$ PFU of virus infectivity but showed limited focal necrosis at day 7 p.i. (Fig. 1A) and virus replication (by in situ hybridization) at day 4 p.i. (Fig. 2D). To further examine this apparent contradiction, popliteal LNs from three anti-IFN-γ-treated and three untreated mice infected with EV were harvested at day 6 p.i. and prepared for electron microscopy.

Electron microscopy. Evaluation of ultrastructural changes confirmed impressions gained from results with light microscopy and in situ hybridization. The draining popliteal LNs from B6 mice given anti-IFN-γ were extensively necrotic with a few viable lymphoid cells and macrophages scattered through remnants of the fibroreticular cells (Fig. 3A and B). These cells were widely separated because of the extreme edema seen in necrotic nodes. Endothelial and fibroreticular cells were recognizable, but both had undergone degeneration. Mature virions (Fig. 3B, small white arrows) were visible within the fibroreticular cells or enmeshed in cytoplasmic fragments of degenerated cells but were absent in endothelial cells, macrophages, and the few lymphoid cells present. In B6 mice which had not been given anti-IFN-γ, there were relatively few signs suggestive of previous EV-induced pathologic changes, most notably the presence of neutrophils (Fig. 3C and D) and activated macrophages containing phagosomes filled with amorphous material (Fig. 3D). Many intact lymphoid cells were present, but mitotic figures among them were rare, indicating exogenous origin. No virus-infected cells or free virions were detected, suggesting that virus replication within the popliteal LNs was an infrequent event and confirming the lack of correlation between the amount of recoverable virus and tissue destruction of the popliteal LNs. Therefore the virus infectivity detected at day 14 p.i. (Table 2) was probably not due to widespread virus replication in the LNs but, rather, to the trapping of EV virions delivered by the afferent lymphatics from the f.p.

Flow microfluorometry analysis of splenocytes from mice 5 days after EV infection. To determine whether treatments of EV-infected mice with the various anti-IFN antibodies had any effect on the splenic leukocyte yield or frequency of specific cell lineages, spleen cell populations from mice sacrificed on day 5 p.i. were analyzed by flow microfluorometry.

The yield of viable leukocytes in the spleen was not altered after treatment with the different anti-IFN antibodies in uninfected mice (Table 5, compare group A with groups B to E). Infection with EV (group F) resulted in a twofold increase in the number of leukocytes compared with that in spleens from uninfected mice (group A) or uninfected and antibody-treated mice (groups B to E). There was also no difference in splenocyte yields from EV-infected mice following treatment with control IgG (groups G and H), rabbit preimmune serum (group I), anti-IFN-αβ (group J), or anti-

FIG. 1. Light-microscopic evaluation of tissue from EV-infected and anti-IFN-treated C57BL/6 mice. B6 mice were infected and treated as described in Materials and Methods. At day 7 p.i. the mice were sacrificed and the draining popliteal LNs, liver, lungs, and spleen were harvested and treated for histopathological examination (see Materials and Methods). (A) Draining popliteal LN from mouse 1684 (no treatment; Table 4) showed an area of necrosis which was restricted to the subcapsular cortical area. Perinodal adipose tissue (upper right) was infiltrated with inflammatory cells. The subcapsular sinusoid was filled with material which may be fibrin. Neutrophils constitute the major inflammatory cell in the underlying area of necrosis. The intact, reactive remainder of the node was sharply demarcated from the necrotic cortex. Bar, 20 μm. (B) Draining popliteal LN from mouse 1692 (anti-IFN-β treatment) depicted confluent necrosis (left-hand portion defined by arrows) which was more extensive than for mouse 1684. The intact medulla was reactive with plasma cells and immunoblasts within the cords. Infiltration of the adipose tissue (lower left) surrounding the node reflected the widespread inflammation associated with EV inoculation in the f.p. Bar, 100 μm. (C) Completely necrotic popliteal LN from mouse 1691 (anti-IFN-β treatment). Bar, 50 μm. (D) A focus of necrosis with moderate infiltration of mononuclear cells in the liver of mouse 1694 (anti-IFN-γ treatment) was sharply delineated (arrows) from the surrounding intact hepatic parenchyma. Bar, 20 μm. (E) Extensive necrosis, involving almost all hepatocytes, was observed in the liver of mouse 1693 (anti-IFN-γ treatment). Note the absence of inflammatory-cell infiltration and pooling of erythrocytes at upper right and lower left (arrows). Bar, 20 μm. (F) Spleen from mouse 1693 (anti-IFN-γ treatment) showing necrosis and complete destruction of the splenic architecture. Bar, 20 μm.

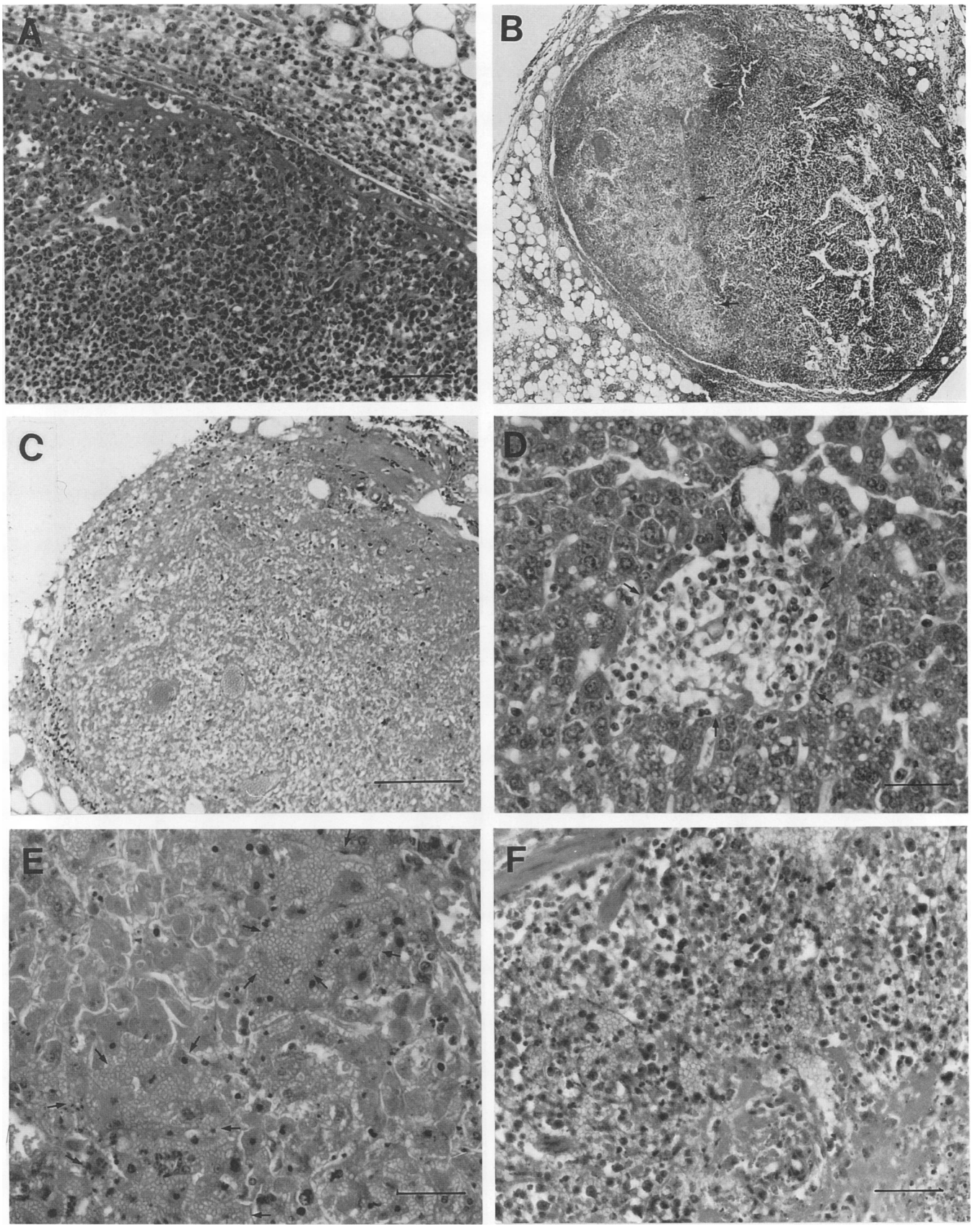
A
B
C
D
E
F

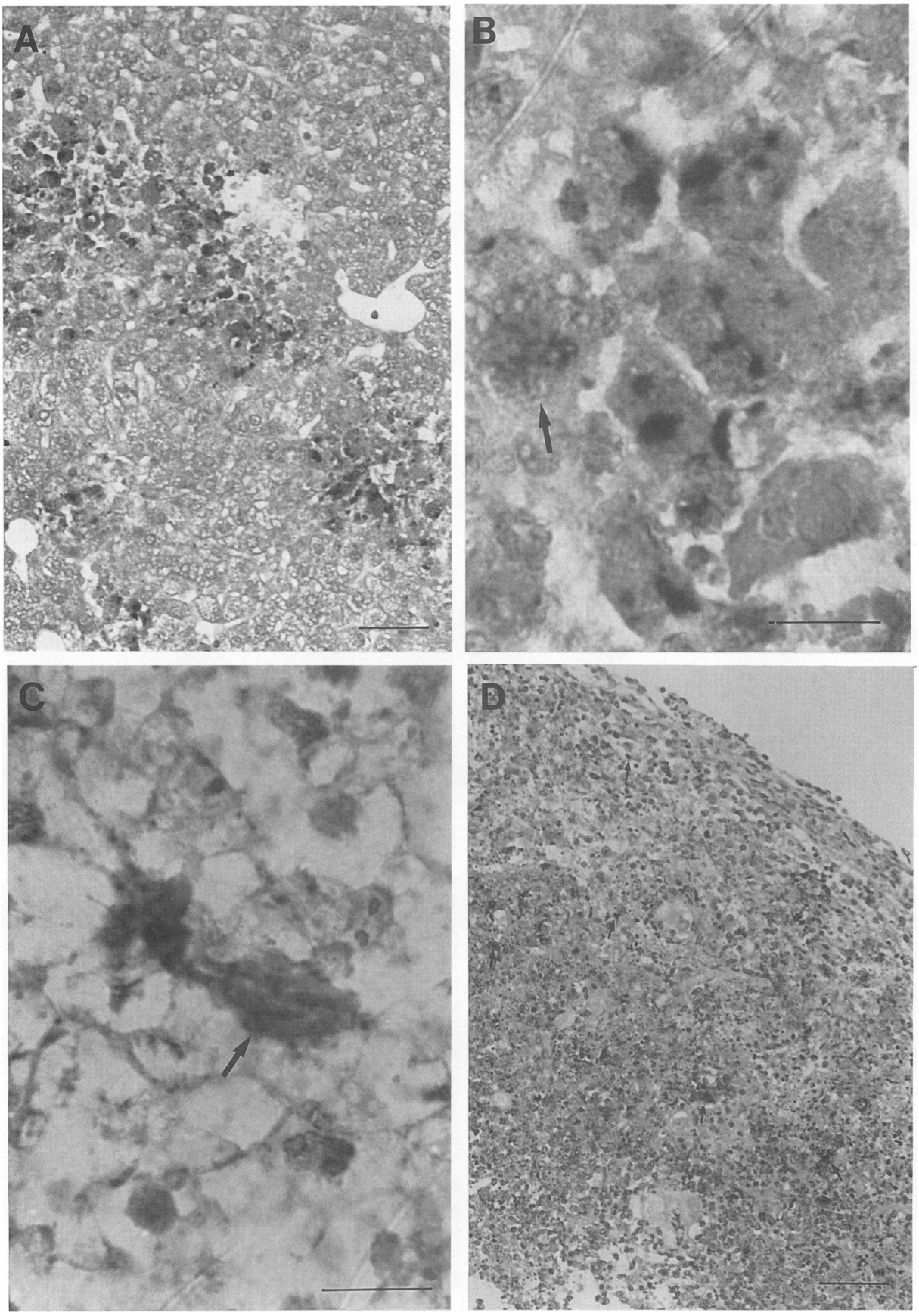
A
B
C
D

IFN-β (group K); however, treatment of infected B6 mice with either of the anti-IFN-γ antibodies resulted in smaller spleens and a 2- to 3.5-fold reduction in viable splenocyte yields (groups L and M) compared with the responses of mice given virus alone (group F).

Flow-cytometric analysis revealed no significant differences in the proportion of T cells, B cells, and Mac-1^+ cells (macrophages and granulocytes) in uninfected mice, whether or not they had been treated with any of the antibodies. The only significant differences in splenic populations from untreated infected mice and uninfected mice were increases in the percentage of γδ-TCR^+ cells (4.9% in infected mice compared with 1.7% in uninfected mice) and Mac-1^+ cells (11.6% in infected mice compared with 3.5% in uninfected mice). Treatment of infected mice with control IgG or preimmune serum gave a pattern essentially identical to that for untreated, infected mice (compare groups G to I with group F). Compared with the control infections, both anti-IFN-αβ and anti-IFN-β treatments did cause a slight reduction in the percentage of αβ-TCR^+ (6 to 8%) and γδ-TCR^+ (2 to 2.5%) cells and a concomitant reduction in the percentage of $CD3^+$ (7 to 8%) cells. No changes were noted in the B-cell population.

In contrast, significant reductions in the T- and B-cell populations were noted in spleens of mice infected with virus and treated with either rat or rabbit anti-IFN-γ antibody compared with the results with controls. Reductions were noted in the percentage of all markers except the percentage of Mac-1^+ cells, which doubled in these mice compared with the level in mice infected with virus only or treated with control IgG, rabbit preimmune serum, anti-IFN-αβ, or anti-IFN-β. The data indicated clearly that depletion of IFN-γ, but not IFN-α and/or IFN-β, resulted in a significant reduction in the number of viable splenocytes and a concomitant decrease in the frequency of T (especially the cells bearing the γδ-TCR) and B cells but not in Mac-1^+ cells, although in absolute numbers Mac-1^+ cells were also reduced compared with control values. The large increase in the numbers of γδ-TCR^+ cells following EV infection and the sensitivity of this response to anti-IFN-γ treatment deserve further study.

Effect of anti-IFN antibody treatment on NK responses. IFNs are potent activators of NK cells (43), which also produce a variety of antiviral cytokines such as IFN-α, IFN-β, and IFN-γ, depending on the nature of the activation stimuli. Since NK cells may be important for the control of virus replication early during infection, it was important to determine whether depletion of IFNs in vivo with antibodies inhibited NK cell cytotoxicity.

Splenocytes obtained from naive or virus-infected mice displayed rather low levels of lysis of YAC-1 targets by days 1 and 3 p.i., and no differences were apparent in antibody-treated and untreated mice (data not shown). Lysis of YAC-1 targets by splenocyte effectors from virus-infected mice sacrificed at day 5 p.i. was more than ninefold higher than levels seen in uninfected controls (Fig. 4A). At the same time, the levels of lysis of YAC-1 cells by effectors from infected mice that had been treated with anti-IFN-αβ, anti-IFN-β, or anti-IFN-γ were approximately threefold lower than the cytolytic activity observed with virus infection alone. The cytolytic activity was mediated by NK cells, since the phenotype of effectors was as-GM_1^+ $CD4^-$ $CD8^-$ Thy-$1.2^\pm$ (data not shown), which is the phenotype of conventional NK cells, and since *H-2*-restricted and virus-specific cytolytic activity (i.e., CTL) was virtually undetected at day 5 p.i.

Effect of anti-IFN antibodies on CTL responses. $CD8^+$ CTL are thought to be crucial for recovery from primary mousepox, and any manipulation in vivo that could impair their generation would also contribute to unchecked virus growth. It was therefore important to establish whether high infectivity levels noted in certain organs after treatment with anti-IFNs correlated with a diminution in the generation of virus-specific CTL responses in vivo. Because the CTL response in infected B6 mice is detectable at day 6 p.i. and peaks between days 7 and 9 p.i., it was necessary to demonstrate any effect of the anti-IFN treatments after day 5 but before any anti-IFN-γ-treated mice died (usually on day 7).

Groups of mice were infected and treated with specific and control antibodies. At day 7 p.i., all mice were sacrificed, organs were removed for virus titration, and spleens were used for determination of CTL activity. No virus was detected in organs from untreated, virus-infected mice, whereas virus infectivity levels in mice which received anti-IFN antibodies were similar to that observed at day 5 in Table 2 (data not shown). The anti-EV CTL responses in spleens from control and antibody-treated, infected B6 mice showed similar levels of killing (Fig. 4B). The phenotype of the *H-2*-restricted, virus-specific killers was Thy-1.2^+ $CD8^+$ $CD4^-$ J11d.2^-.

DISCUSSION

Treatment of EV-infected B6 mice with anti-IFN-γ antibody transformed a mild, inapparent infection into a disease similar to that seen in EV-infected mice with severe combined immunodeficiency, EV-infected athymic mice, or the highly susceptible A strain mice infected with EV (data not shown). The infection was characterized by an early spread of EV from the primary site of replication in the f.p. through the popliteal LN and the lymphatics to the spleen and liver. The lymphoproliferative responses that are normally seen in the popliteal LNs and spleens of infected, untreated B6 mice were absent, and unrestricted virus replication was detected in all organs assayed. The fibroreticular cells of the LN and the hepatocytes of the liver were shown to support virus replication. Uniform mortality was observed by day 7 p.i., which was 2.5 days earlier than EV-induced mortality in untreated, EV-infected mice with severe combined immunodeficiency and was identical with the results obtained with

FIG. 2. In situ hybridization of tissue sections from EV-infected C57BL/6 mice. Mouse 1687 (Table 4) was treated with anti-IFN-αβ prior to and throughout a 7-day infection period, after which it was sacrificed, and tissues were prepared as for histological examination. Sections were processed for in situ hybridization as described in Materials Methods. (A) Discrete areas of hepatic necrosis, similar to those in Fig. 1D, show striking colocalization of the EV DNA probe within areas of hepatic necrosis and absence of viral DNA in unaffected hepatic tissue. Bar, 20 μm. (B) Higher-power micrograph of a necrotic focus showing the diffuse localization (arrow) or the more common focal localization of EV DNA probe within hepatocytes. Bar, 10 μm. (C) Positive cell (arrow) in a necrotic spleen which was generally negative. The positive cells were possibly the fibroreticular cells shown by electron microscopy (Fig. 3B) to be sites of viral replication in the LN. Bar, 10 μm. (D) Area of subcapsular necrosis of an LN from an untreated, infected mouse sacrificed on day 4 p.i. showed that cells reacting with the EV DNA probe (small arrows) were restricted to an area of necrosis and minimally present in more intact areas, as in the lower left. Bar, 20 μm.

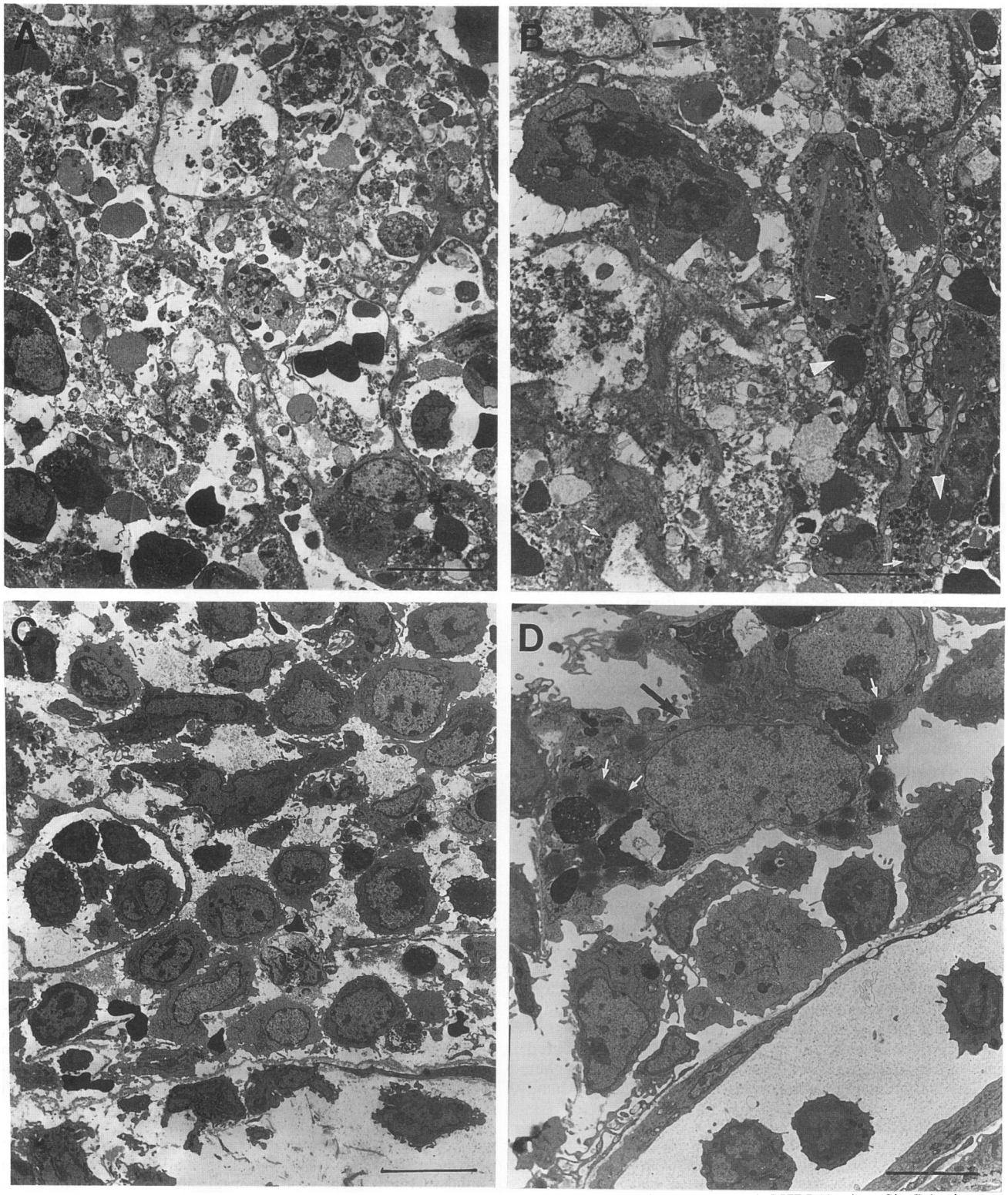

FIG. 3. Electron-microscopic analysis of the popliteal LN from EV-infected and anti-IFN-γ-treated C57BL/6 mice. Six B6 mice were infected in the f.p. with EV. Three were left untreated (mice 1731, 1732, and 1733), and the other three were given anti-IFN-γ antibody (mice 1734, 1735, and 1736), as described in Materials and Methods. On day 6 p.i. the mice were sacrificed and the draining popliteal LNs were harvested and prepared for electron microscopy. (A) Mouse 1736, treated with anti-IFN-γ. The outline of the structural elements of the LN is discernible but shows severe degenerative changes. Components of lysed cells and erythrocytes were suspended within a fluid matrix. Some intact cells remain, including a possible fibroreticular cell at the lower right and several lymphocytes at the lower left. Bar, 10 μm. (B) Mouse 1736, treated with anti-IFN-γ. Three fibroreticular cells (black arrows), identified by fibrillar processes seen particularly clearly in the central

TABLE 5. Flow microfluorometry analysis of splenocytes from C57BL/6 mice 5 days after EV infection

Group[a]	Virus and treatment	Avg lymphocyte yield/spleen ($\times 10^7$)	% of splenocytes positive for:								
			CD4	CD8	αβ-TCR	γδ-TCR	CD3	Thy-1.2	Mac-1	IgM	B220
A	No treatment	6.0	21.3	12.4	33.8	1.7	38.2	32.1	3.5	57.1	59.1
B	Anti-IFN-αβ	6.2	21.8	11.8	32.5	1.6	37.9	30.5	4.1	60.0	62.5
C	Anti-IFN-β	6.6	21.6	12.2	31.5	1.6	35.1	30.6	4.1	58.1	60.4
D	Anti-IFN-γ (rat MAb)	5.6	21.2	10.9	30.9	1.7	36.3	33.5	4.2	58.7	59.7
E	Anti-IFN-γ (rabbit polyclonal)	6.0	21.6	11.9	30.4	1.5	33.8	31.0	5.0	57.4	62.1
F	EV only	12.6	23.3	12.1	35.8	4.9	40.6	35.9	11.6	50.9	58.3
G	EV + rat IgG	11.2	24.9	12.9	36.4	5.7	41.0	35.0	12.0	51.5	57.6
H	EV + rabbit IgG	12.3	24.8	12.5	36.7	4.9	38.4	34.3	11.8	51.0	57.6
I	EV + rabbit Preimmune serum	11.8	23.3	12.8	36.4	4.3	39.0	32.1	9.6	56.4	58.5
J	EV + Anti-IFN-αβ	10.9	20.7	11.9	28.0	2.9	32.6	29.6	12.4	54.5	57.2
K	EV + Anti-IFN-β	11.6	21.4	11.2	29.9	2.5	33.4	28.5	10.0	53.6	61.3
L	EV + Anti-IFN-γ (rat MAb)	3.8	13.1	9.7	22.5	0.5	23.9	25.6	24.9	46.5	47.9
M	EV + Anti-IFN-γ (rabbit polyclonal)	4.5	14.7	10.6	25.6	1.1	27.4	23.7	22.4	46.9	51.1

[a] Groups of four mice were treated as described in Materials and Methods and sacrificed on day 5. Spleens were aspectically removed, and single-cell suspensions were prepared and analyzed as described in Materials and Methods.

the highly susceptible A strain mice (5, 9a). These results were consistent with the conclusion that IFN-γ has an important role in controlling virus replication throughout the infection process and especially in the draining popliteal LNs. The potential lymphocyte populations involved in early production of IFN-γ are NK cells, and γδ-TCR$^+$ T cells, which are normally present in the skin, are elevated in the spleens of EV-infected mice and can be activated by virus-induced heat shock proteins (12, 43). With the advent of the virus-specific immune response, both CD4$^+$ and CD8$^+$ T cells would also contribute to the generation of IFN-γ in the infected mice.

IFN-γ could exert its antiviral effect through a number of distinct mechanisms. Although not as efficient as IFN-α or IFN-β, IFN-γ is capable of inducing an antiviral state within potential target cells through the P1/eIF-2α or the 2′,5′-oligo(A) synthetase pathways (32); however, in vitro studies show EV replication to be refractile to the antiviral effects of IFNs, probably because of the presence of homologs of VV open reading frames K3L and E3L (2, 6, 8) and other genes which inhibit these antiviral pathways (data not shown). IFN-γ is also important in the activation of monocytes/macrophages, which are known to be important in recovery from EV infection (3, 39). Furthermore, since IFN-γ regulates the expression of adhesion molecules and ligands (37), the induction of major histocompatibility complex class I and II cell surface molecules (30), and the processing and presentation of viral peptides by infected cells to effector T cells (29, 33, 45), it is probably important for inflammatory-cell and CD8$^+$ T-cell diapedesis into infected tissue and T-cell recognition of infected cells.

The extremely high levels of EV infectivity at days 5 to 7 p.i. in tested tissues suggested that CTL were not efficiently eliminating virus-infected cells, although depletion of IFN-γ (or other IFNs) in vivo had no dramatic effect on the generation and cytolytic activity (measured in vitro) of anti-ectromelia virus-specific CTL. This observation was consistent with results of other studies, which found that IFN-γ depletion in vivo had no adverse effects on anti-vesicular stomatitis virus (20) or anti-VV (15, 31) CTL generation but did affect the clearance of lymphocytic choriomeningitis virus (17, 20, 44) and murine cytomegalovirus (21) from infected mouse spleens and salivary glands, respectively. In fact, for VV, depletion of IFN-γ actually enhanced the anti-VV CTL response (15). Since VV does not replicate efficiently in the mouse, the enhanced anti-VV CTL response was attributed to increased virus replication and hence an increased antigenic load (15). In the present study, the slight reduction in cytolytic activity in anti-IFN-γ-treated animals could be the result of a reduction in the number of CD8$^+$ T cells or CD4$^+$ helper T cells, which may be important in optimal CD8$^+$ CTL generation under conditions of greater antigenic burden, which would exist in anti-IFN-γ-treated mice (12a). CD4$^+$ T cells have been shown not to be important in recovery from mousepox or in the generation of a CTL response under normal conditions (4). This result could also be explained by the direct or indirect cytopathic effect of a 4- to 6-$\log_{10}$ unit increase in virus infectivity in the spleens of IFN-γ-treated mice compared with controls. Collectively, these studies do not support a role for IFNs in the in vivo generation of CTL; however, they cannot rule out a role for IFNs which may be secreted locally into the limited space between interacting cell types (27) or used in an autocrine manner.

To a lesser extent, IFN-β also appeared to be important for recovery from mousepox and especially crucial for virus clearance in the liver and ovaries. Because an antibody to IFN-α was unavailable, the importance of IFN-α in virus

cell, contained large numbers of mature virions (white arrows) as well as inclusion bodies (white arrowheads). In contrast, the macrophage at the upper left did not contain virions. The rest of the node was filled with debris, erythrocytes, and possibly fibrin in which virions were trapped (lower left). Bar, 5 μm. (C) Mouse 1734, no anti-IFN-γ. The structural components of the lymph node appeared intact, with little evidence of cellular necrosis. The most notable change was the separation of the cells within the LN as a result of edema and the presence of neutrophils in addition to lymphoid cells and macrophages. No free virions or cells showing active virus replication were present. Mitotic figures among the cells within the node were rare. Bar, 10 μm. (D) Mouse 1732, no anti-IFN-γ. The capillary containing neutrophils was intact. A binucleated macrophage (black arrow) had numerous phagocytic vacuoles (small white arrows), but note the absence of virions either within cells or in the extracellular space, which were clear of any debris. Bar, 5 μm.

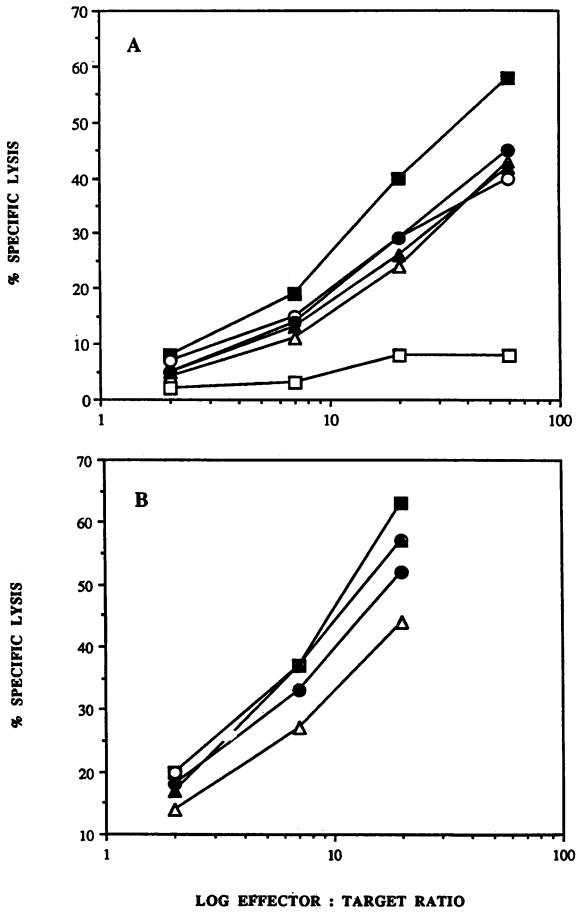

FIG. 4. Effect of anti-IFN treatments on NK cell and CTL responses. Groups of three B6 mice were inoculated with or without EV by the f.p. route in combination with various antibody treatments as described in Materials and Methods. At day 5 (NK responses) (A) or day 7 (CTL responses) (B) p.i., spleen cells from mice in each treatment group were pooled and the capacity of the splenocytes to lyse ^{51}Cr-labeled YAC-1 targets (panel A) or VV-infected *H-2*-compatible MC-57G cells (panel B) was measured. Symbols: □, spleen cells from uninfected, untreated mice; ■, spleen cells from virus-infected, untreated mice; ○, spleen cells from mice infected and treated with anti-IFN-αβ; ●, spleen cells from mice infected and treated with anti-IFN-β; △, spleen cells from mice infected and treated with rat anti-IFN-γ; ▲, spleen cells from mice infected and treated with rabbit anti-IFN-γ. Two of the three mice infected with virus and given rabbit polyclonal antibody to murine IFN-γ died just prior to sacrifice, so the CTL activity was determined by using a single spleen. The assay was carried out in triplicate for each effector-to-target cell ratio, and the standard errors of the mean were less than 5%. In panel A, the levels of YAC-1 target cell lysis caused by splenocytes from uninfected mice that were receiving antibody treatments were not significantly different from lysis due to splenocytes from uninfected, untreated controls and therefore have been omitted for clarity. In panel B, lysis values are expressed as ^{51}Cr release from infected MC-57G targets minus uninfected MC-57G target cells, which were 10 to 30% of the former values.

clearance had to be determined by comparing the effects of anti-IFN-αβ and anti-IFN-β. This approach did not support an important role for IFN-α in virus clearance. Because the type I and type II IFNs often act in synergy to produce potent virus-inhibitory action (10, 46), the removal of one (as done here) of the synergistic pair will invariably affect the efficacy of the antiviral activity of the other. Our data suggest that both type I (IFN-β) and type II (IFN-γ) IFNs are important for virus clearance in the liver and ovaries since depletion of either of them results in enhanced virus replication and virus persistence. On the other hand, virus infectivity levels in lung and spleen tissue of EV-infected mice treated with anti-IFN-β differed from control levels only at day 5 p.i. The differential importance of IFN species for the control of virus replication in particular tissues may be a reflection of distinct differences in production of IFNs in the microenvironment, the ability of the virus-encoded functions to abrogate IFN action, or a failure of the rabbit polyclonal antibody to IFN-β to traffic as efficiently as the rat anti-IFN-γ MAb to lung and spleen tissue (38). This last possibility could explain the results with the lung tissue, since infected B6 mice treated with rabbit polyclonal anti-IFN-γ had a 1.7 $\log_{10}$ PFU lower infectivity level in lung tissue than in comparable samples from B6 mice treated with rat MAb against IFN-γ; however, differential trafficking of antibody cannot explain the failure of EV to replicate to high levels of infectivity in the spleen, since enhanced virus replication was observed in spleen, liver, and ovary tissue from EV-infected mice treated with either a rabbit polyclonal antibody or a rat MAb to IFN-γ (data not shown).

The persistence of high levels of virus infectivity in the f.p. (until at least day 14 p.i.) suggests that this primary site of EV replication is protected from antiviral host defense mechanisms, including the antiviral CTLs, which reach peak levels at day 8 p.i. in the spleen and are thought to be the major means of virus clearance from internal organs (5, 9a). Also, there was a failure of the anti-IFN antibodies directly administered to the f.p. to increase dramatically virus replication in the f.p., which is consistent with EV-encoded homologs of the VV open reading frames K3L and E3L (2, 6, 8) blocking the IFN-induced anti-viral state. By analogy to other poxviruses, the protection of this primary site of EV replication from host defense mechanisms could be further enhanced by a soluble TNF receptor, which in Shope fibroma virus (34) and myxoma virus (40) infections binds TNF-α and-β; a soluble interleukin-1 receptor, which in VV infections binds to and blocks the action of interleukin-1β (1, 36); a soluble IFN-γ receptor, which in Shope fibroma virus and myxomavirus infections binds to and blocks the action of IFN-γ (41); a complement control protein, which in VV infections has been shown to block antibody-dependent activation of the complement cascade via the classical or alternative pathways (19); and a 38-kDa protein, which acts as a potent anti-inflammatory agent in cowpox virus infections of the chicken embryo (25, 25a, 28). This persistence of high levels of virus infectivity in the f.p. is undoubtedly important in the highly efficient transmission of EV from infected B6 index mice to cage mates between days 8 and 14 p.i. (42).

As shown in this study, IFN-γ appears to be a crucial cytokine for recovery from infection and appears to have both an early as yet undefined role and a later function within the context of CTL-mediated virus clearance. Further studies should focus on determining whether IFN-γ is the radioresistant factor(s) involved in the early mechanism of resistance to mousepox and the role of NK cell-secreted IFNs in recovery from EV-infection. In addition, the possibility that susceptibility to severe mousepox is correlated to genetic defects in IFN-γ production or action is being investigated.

ACKNOWLEDGMENTS

We thank A. Anderson for advice regarding interpretation of morphologic changes within the LN; G. Palumbo for critical review of the manuscript; B. R. Marshall, Sharon Chambers, and Thomas Oommen for expert manuscript preparation; C. Duarte and Lynn Budgeon for technical assistance; and B. Moss for continued support.

REFERENCES

1. **Alcami, A., and G. L. Smith.** 1992. A soluble receptor for interleukin-Iβ encoded by vaccinia virus: a novel mechanism of virus modulation of the host responses to infection. Cell **71**:153–160.
2. **Beattie, E., J. Taraglia, and E. Paoletti.** 1991. Vaccinia virus-encoded eIF-2α homolog abrogates the antiviral effect of interferon. Virology **183**:419–422.
3. **Blanden, R. V.** 1982. Role of macrophages in elimination of viral infection, p. 269–278. *In* D. Mizuno, Z. A. Cohn, K. Takeya, and N. Ishida (ed.), Self defense mechanisms: role of macrophages. University of Tokyo Press, Elsevier Biomedical Press, Tokyo.
4. **Buller, R. M. L., K. L. Holmes, A. Hugin, T. N. Frederickson, and H. C. Morse III.** 1987. Induction of cytotoxic T cell response *in vivo* in the absence of $CD4^+$ helper cells. Nature (London) **328**:77–79.
5. **Buller, R. M. L., and G. J. Palumbo.** 1991. Poxvirus pathogenesis. Microbiol. Rev. **55**:80–122.
6. **Chang, H.-W., J. C. Watson, and B. L. Jacobs.** 1992. The E3L gene of vaccinia virus encodes an inhibitor of the interferon-induced, double-stranded RNA-dependent protein kinase. Proc. Natl. Acad. Sci. USA **89**:4825–4829.
7. **Chen, W., R. Drillien, D. Spehner, and R. M. L. Buller.** 1992. Restricted replication of ectromelia virus in cell culture correlates with mutations in virus-encoded host range gene. Virology **187**:433–442.
8. **Davies, M. V., O. Elroy-Stein, R. Jagus, B. Moss, and R. J. Kaufman.** 1992. The vaccinia virus K3L gene product potentiates translation by inhibiting double-stranded-RNA-activated protein kinase and phosphorylation of the α subunit of eukaryotic initiation factor 2. J. Virol. **66**:1943–1950.
9. **Fenner, F.** 1949. Mousepox (infectious ectromelia of mice): a review. J. Immunol. **63**:341–373.

9a. **Fenner, F., R. Wittek, and K. R. Dumbell.** 1989. The orthopoxviruses. Academic Press, Inc., San Diego, Calif.

10. **Fleischmann, W. R., Jr., C. C. Fleischmann, and W. Fiers.** 1984. Potentiation of interferon action by mixtures of recombinant DNA-derived human interferons. Antiviral Res. **4**:357–360.
11. **Jacoby, R. O., P. N. Bhatt, and D. G. Brownstein.** 1989. Evidence that NK cells and interferon are required for genetic resistance to lethal infection with ectromelia virus. Arch. Virol. **108**:49–58.
12. **Jindal, S., and R. A. Young.** 1992. Vaccinia virus infection induces a stress response that leads to association of Hsp70 with viral proteins. J. Virol. **66**:5357–5363.

12a. **Karupiah, G., and R. Blanden.** Unpublished observations.

13. **Karupiah, G., R. V. Blanden, and I. A. Ramshaw.** 1990. IFN-γ is involved in the recovery of athymic nude mice from recombinant vaccinia virus/IL-2 infection. J. Exp. Med. **172**:1495–1503.
14. **Karupiah, G., B. E. H. Coupar, M. E. Andrew, D. B. Boyle, S. M. Phillips, A. Müllbacher, R. V. Blanden, and I. A. Ramshaw.** 1990. Elevated NK cell responses in mice infected with recombinant vaccinia virus encoding murine IL-2. J. Immunol. **144**:290–298.
15. **Karupiah, G., C. E. Woodhams, R. V. Blanden, and I. A. Ramshaw.** 1991. Immunobiology of infection with recombinant vaccinia virus encoding murine IL-2. Mechanisms of rapid viral clearance in immunocompetent mice. J. Immunol. **147**:4327–4332.
16. **Kees, U. R., and R. V. Blanden.** 1976. A single genetic element in H-2K affects mouse T cell antiviral function in poxvirus infection. J. Exp. Med. **143**:450–456.
17. **Klavinskis, L. S., R. Geckeler, and M. B. A. Oldstone.** 1989. Cytotoxic T lymphocyte control of acute lymphocytic choriomeningitis virus infection: interferon γ, but not tumor necrosis factor α, displays antiviral activity in vivo. J. Gen. Virol. **70**:3317–3325.
18. **Kohonen-Corish, M. R. J., N. J. C. King, C. E. Woodhams, and I. A. Ramshaw.** 1990. Immunodeficient mice recover from infection with vaccinia virus expressing interferon-γ. Eur. J. Immunol. **20**:157–161.
19. **Kotwal, G. J., S. N. Isaacs, and B. Moss.** 1990. Inhibition of the complement cascade by the major secretory protein of vaccinia virus. Science **250**:827–830.
20. **Leist, T. P., M. Eppler, and R. M. Zinkernagel.** 1989. Enhanced virus replication and inhibition of lymphocytic choriomeningitis virus disease in anti-gamma interferon-treated mice. J. Virol. **63**:2813–2819.
21. **Lučin, P., I. Pavić, B. Polić, S. Jonić, and U. Koszinowski.** 1992. Gamma interferon-dependent clearance of cytomegalovirus infection in salivary glands. J. Virol. **66**:1977–1984.
22. **O'Neill, H. C., and R. V. Blanden.** 1983. Mechanisms determining innate resistance to ectromelia virus infection in C57BL mice. Infect. Immun. **41**:1391–1394.
23. **O'Neill, H. C., R. V. Blanden, and T. J. O'Neill.** 1983. H-2-linked control of resistance to ectromelia virus infection in B10 congenic mice. Immunogenetics **18**:255–265.
24. **O'Neill, H. C., and M. Brenan.** 1987. A role for early cytotoxic T cells in resistance to ectromelia virus infection in mice. J. Gen. Virol. **68**:2669–2673.
25. **Palumbo, G. J., W. C. Glasgow, and R. M. L. Buller.** 1993. Poxvirus-induced alteration of arachidonate metabolism. Proc. Natl. Acad. Sci. USA **90**:2020–2024.

25a. **Palumbo, G. J., D. J. Pickup, T. N. Fredrickson, L. J. McIntyre, and R. M. L. Buller.** 1989. Inhibition of an inflammatory response is mediated by a 38-kDa protein of cowpox virus. Virology **172**:262–273.

26. **Pestka, S., J. A. Langer, K. C. Zoon, and C. E. Samuel.** 1987. Interferons and their actions. Annu. Rev. Biochem. **56**:727–777.
27. **Poo, J.-J., L. Conrad, and C. A. Janeway.** 1988. Receptor-directed focusing of lymphokine release by helper T cells. Nature (London) **332**:378–380.
28. **Ray, C. A., R. A. Black, S. R. Koronheim, T. A. Greenstreet, P. R. Sleath, G. S. Salvesen, and D. J. Pickup.** 1992. Viral inhibition of inflammation: cowpox virus encodes an inhibitor of the interleukin-1β converting enzyme. Cell **69**:597–604.
29. **Robertson, M.** 1991. Antigen processing: proteosomes in the pathway. Nature (London) **353**:300–301.
30. **Rosa, F., D. Hatat, A. Abadie, and M. Fellous.** 1985. Regulation of histocompatibility antigens by interferon. Ann. Inst. Pasteur Immunol. **136C**:103–119.
31. **Ruby, J., and I. Ramshaw.** 1991. The antiviral activity of immune $CD8^+$ T cells is dependent on interferon-γ. Lymphokine Cytokine Res. **10**:353–358.
32. **Samuel, C. E.** 1991. Antiviral actions of interferon. Interferon-regulated cellular proteins and their surprisingly selective antiviral activities. Virology **183**:1–11.
33. **Sibille, C., K. Gould, G. Hämmerling, and A. Townsend.** 1992. A defect in the presentation of intracellular viral antigens is restored by interferon-γ in cell lines with impaired major histocompatibility complex class I assembly. Eur. J. Immunol. **22**:433–440.
34. **Smith, C. A., T. Davis, D. Anderson, L. Solam, M. P. Beckmann, R. Jezy, S. K. Dower, D. Cosman, and R. G. Goodwin.** 1990. A receptor for tumor necrosis factor defines an unusual family of cellular and viral proteins. Science **248**:1019–1023.
35. **Spitalny, G. L., and E. A. Havell.** 1984. Monoclonal antibody to murine γ interferon inhibits lymphokine-induced antiviral and macrophage tumoricidal activities. J. Exp. Med. **159**:1560–1565.
36. **Spriggs, M. K., D. Hruby, C. R. Maliszewski, D. J. Pickup, J. E. Sims, R. M. L. Buller, and J. Van Slyke.** Vaccinia and cowpox viruses encode a novel secreted interleukin-1-binding protein. Cell **71**:145–152.
37. **Springer, T. A.** 1990. Adhesion receptors of the immune system. Nature (London) **346**:425–434.
38. **Stein-Streilein, J., and J. Guffee.** 1986. In vivo treatment of mice

and hamsters with antibodies to asialo GM_1 increases morbidity and mortality to pulmonary influenza infection. J. Immunol. **136:**1435–1440.

39. **Tsuru, S., H. Kitani, M. Seno, M. Abe, Y. Zinnaka, and K. Nomoto.** 1983. Mechanism of protection during the early phase of a generalized viral infection. I. Contribution of phagocytes to protection against ectromelia virus. J. Gen. Virol. **64:**2021–2026.
40. **Upton, C., J. L. Macen, M. Schreiber, and G. McFadden.** 1991. Myxoma virus expresses a secreted protein with homology to the tumor necrosis factor receptor gene family that contributes to viral virulence. Virology **184:**370–382.
41. **Upton, C., K. Mossman, and G. McFadden.** 1992. Encoding of a homolog of the IFN-γ receptor by myxoma virus. Science **258:**1369–1372.
42. **Wallace, G. D., and R. M. L. Buller.** 1985. Kinetics of ectromelia virus (mousepox) transmission and clinical response in C57BL/6J, BALB/cByJ and AKR/J inbred mice. Lab. Anim. Sci. **35:**41–46.
43. **Welsh, R. M.** 1984. Natural killer cells and interferon. Crit. Rev. Immunol. **5:**55–93.
44. **Wille, A., A. Gessner, H. Lother, and F. Lehmann-Grube.** 1989. Mechanism of recovery from acute virus infection. VIII. Treatment of lymphocytic choriomeningitis virus-infected mice with anti-interferon γ monoclonal antibody blocks generation of virus-specific cytotoxic T lymphocytes and virus elimination. Eur. J. Immunol. **19:**1283–1288.
45. **Yang, Y., J. B. Waters, K. Früh, and P. A. Peterson.** 1992. Proteasomes are regulated by interferon γ. implications for antigen processing. Proc. Natl. Acad. Sci. USA **89:**4928–4932.
46. **Zerial, A., A. G. Hovanessian, S. Stefano, K. Huygen, G. H. Werner, and E. Falcoff.** 1982. Synergistic activities of type I (α,β) and type II (γ) murine interferon. Antiviral Res. **2:**227–239.